ELSEVIER

Journal of Crystal Growth 170 (1997) 710–714

JOURNAL OF CRYSTAL GROWTH

Temperature dependence on the emerging crystal habit of GaInP deposited on nonplanar {001}GaAs substrates

P.L. Bastos *, M.J. Anders, M.M.G. Bongers, P.R. Hageman, L.J. Giling

Department of Experimental Solid State Physics III, Research Institute of Materials, University of Nijmegen, 6525 ED Nijmegen, The Netherlands

Abstract

In this study the low-pressure (20 mbar) organometallic vapour phase epitaxy (LP-OMVPE) of GaInP on nonplanar {001} GaAs substrates has been examined in the 640°C–760°C temperature range. Growth of this alloy on these surfaces can be characterized by low and high temperature regimes. At low temperatures ($T < 720$°C) the growth rate difference, between the planar and the nonplanar side walls, are large, and faceting features appear along the bottom corners and top edges. At the higher temperatures ($T \geq 720$°C) these facets are no longer present and the intra-cavity deposition profile follows the contour of the groove. These results have been compared to computer simulations of surface concentration profiles whereby the inversely proportional relation between temperature and supersaturation, along with varying growth rate on adjacent surfaces of different crystallographic orientations, is found to be the driving force behind the occurrence of these features. The stability of the observed facets is related to the decrease in dangling bond densities upon surface reconstruction.

1. Introduction

The large bandgap difference between ordered and disordered GaInP makes this alloy an interesting candidate for disordered–ordered–disordered (DOD) systems where low dimensional quantum confinement can be explored. The bandgap engineering of this unicompositional structure would be an alternative to other systems, such as GaAs/GaInP, where intermixing of the group V component occurs along the heterointerface [1,2].

Low dimensional confinement of compound semiconductors may also be achieved on patterned surfaces producing a host of structures such as quantum: wires [3,4], dots [5,6] and wire lasers [7–9].

The emerging crystal habit plays an integral role in the growth profile form which will influence the desired function. Faceting can develop and be either a detrimental feature causing discontinuities in the deposited layer or beneficial in development of the aforementioned nanostructures. The primary motivation for this study was to examine the fundamental aspects of facet formation during the nonplanar LP-OMVPE of GaInP as related to temperature, supersaturations and growth rates along the nonplanar surfaces with respect to the uppermost {001} surfaces.

2. Experimental procedure

The inverted mesa (IMG) and dovetail grooves (DG) were obtained by conventional photolithogra-

* Corresponding author. Fax: +31 24 365 2314.

PII S0022-0248(96)00501-5

phy and wet chemical etching – i.e. 4:1:5 and 1:8:1 solutions respectively of $H_2SO_4:H_2O_2:H_20$, on (001), 2° misoriented towards the ⟨110⟩, GaAs substrates. The generated patterns consisted of: 5 to 100 μm wide stripes, etched to a depth of 10 to 15 μm along ⟨110⟩ and its orthogonal ⟨1$\bar{1}$0⟩ direction, with an inter-stripe separation length of 300 μm. Planar surfaces, with comparable crystallographic orientations ((001), {111}A/B and (110)) to those encountered along the side walls of the aforementioned cavities, were also used along with the nonplanar substrates in order to compare the patterned with the unpatterned results. The contrast between planar and nonplanar growth, compositional variations across the encountered faces and details of the DG are subject matters that will be thoroughly addressed in a forthcoming study [10].

The growth parameters were chosen as such in order to produce nominally lattice matched ($x = 0.517$) compositions of $Ga_xIn_{1-x}P$ on {001} surfaces across the 640°C–760°C, by 40°C increments, temperature range. The group V hydride source consisted of 100% arsine and phosphine and the group III organometallic precursors were made up of trimethylalkyls of gallium and indium. The growth rate, V/III ratio, total reactor pressure and flow rate were: 1 to 2 μm/h, 400, 20 mbar, and 7 l/min of mainly palladium purified hydrogen carrier gas, respectively.

The grown structure consisted of a 0.1 μm GaAs buffer layer, with respect to the {001} surfaces, followed by one to two hours of growth of the ternary alloy. Cleaved cross sections, along the ⟨1$\bar{1}$0⟩ directions (Fig. 1), were examined by scanning electron microscopy (SEM) in order to determine layer thicknesses, surface structures and the development of facets within the groove. Nomarski microscopy was also used in order to evaluate surface morphologies.

3. Results and discussion

The primary finding was that for $T \leq 720$°C $\{\bar{h}\bar{h}k\}_{k>h}$ facets ({$\bar{1}\bar{1}$3}A and {$\bar{1}\bar{1}$5}A), emanating from the bottom corner of the IMG (Fig. 1), were observed. The criterion for the disappearance of these features was found to be related to the higher temperature deposition ($T \geq 720$°C) were the relative

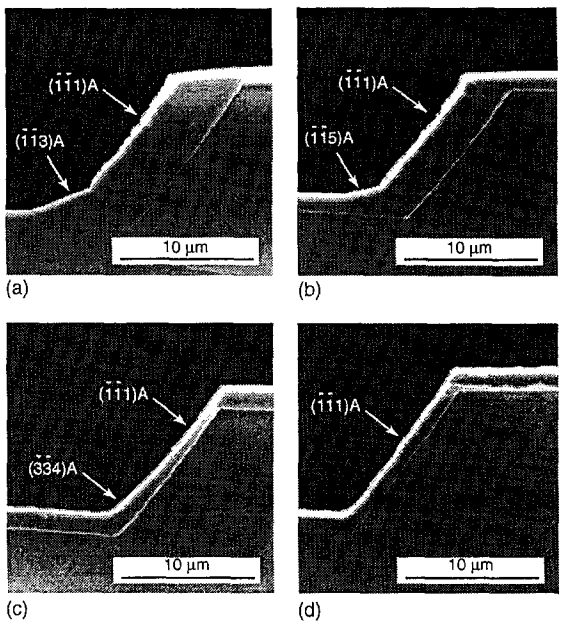

Fig. 1. Scanning electron micrograph of {1$\bar{1}$0} cross sections of GaInP deposition on inverted mesa grooves (IMG) at (a) 640°C, (b) 680°C, (c) 720°C and (d) 760°C.

growth rates – i.e. growth rates normalized to the nearest {001} plane – are near unity (Fig. 2).

These results where correlated to computer simulations of the surface concentration across the various nonplanar geometries [11]. The model uses the relative growth rate results (Fig. 2) in a dimensionless analysis based on mass balance of Fickian diffusion everywhere along with surface reaction kinetic fluxes taken to be proportional to the surface concentration. The characteristic features of these profiles is that the surface concentration is enhanced near the top edge and that the intra-cavity profile is inversely proportional to temperature (Fig. 3). At low temperatures ($T < 720$°C), the intra-cavity supersaturations is "valley" (concave) shaped. As the temperature increases ($T \geq 720$°C) the groove's surface concentration decreases (Fig. 2) and the profile becomes "hill" (convex) shaped [11].

The overall implication of the proposed model [11] is that the edge protrusions and intra-cavity concentration profile are due to the temperature dependent gas phase diffusion along nonplanar surfaces. There will be a flux of growth species through the gas phase from one facet to another in order to

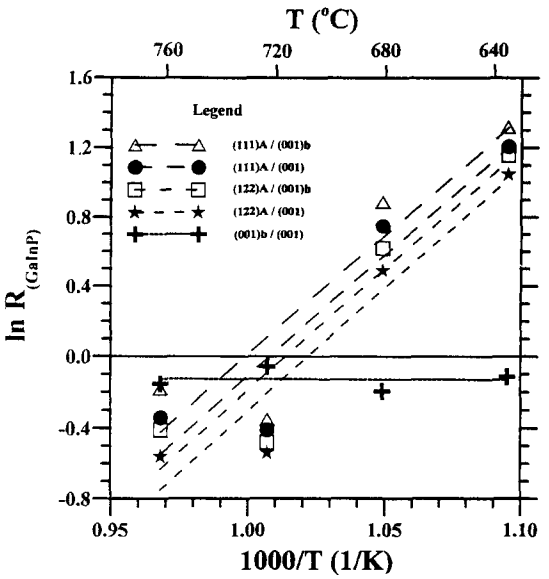

Fig. 2. Relative GaInP growth rates on nonplanar surfaces normalized to the nearest {001} plane where "b" denotes the bottom of the cavity.

maintain the dynamic equilibrium of growth across the nonplanar surface [11–13]. This effectively leads to an interplay of growth units from the slower growing surface to an adjacent plane, of different crystallographic orientation with a higher rate of growth.

The bottom corner of the IMG may be envisioned as a macroscopic step. In the low temperature – i.e. higher supersaturation with a "valley" [11] profile (Fig. 3) – impinging growth species, at or near the corner from both the (001) bottom surface and $\{\bar{1}\bar{1}1\}$A side wall, will migrate and attach to these active nucleation sites located along the macroscopic step edge (Fig. 1a and 1b). The formation of the bottom corner $\{\bar{h}\bar{h}k\}A_{k>h}$ faceting features are primarily a result of the higher surface concentration of the growth species at these corners. Although the formation of these corner facets occurs at the onset of growth they follow the transformation of the IMG into the V grooves (VG) configuration – not shown for the sake of brevity – in a more or less unchanged manner until they are buried as the groove begins to fill and eventually becomes coplanar with the uppermost {001} surface. In this low temperature high supersaturation regime the corner faceting features, bounded by the $\{\bar{1}\bar{1}1\}$A side wall and the lower {001} surfaces, will, in addition to the gas phase concentration profile, also develop as a consequence of the local surface transport of species from an adjacent face with a lower rate of growth such as the groove's {001} bottom.

At higher temperature, lower supersaturation, regime the surface concentration profile is "hill" [11] shaped (Fig. 3). For this case deposition on the {001} bottom surface will predominantly occur from the impingement of growth species onto the middle section of the plane and extend, due to higher surface mobilities, laterally towards the edges where the concentration profile is lower. The lower relative growth rate values (Fig. 2) indicate that both the bottom surface and side walls are growing at similar rates, therefore, the accumulation of excess species along the bottom corners is less likely to occur. Under these conditions the filling of the groove is characterized as being uniform and without the $\{\bar{h}\bar{h}k\}A_{k>h}$ faceting features (Fig. 1c and 1d).The encountered $\{\bar{h}\bar{h}k\}A_{k>h}$ ($\{\bar{1}\bar{1}3\}$A $\{\bar{1}\bar{1}5\}$A) faceting features, located at the bottom corner of the IMG (Fig. 1a and 1b), are stepped structures consisting of {001} treads and {111} risers [16]. Along this concave geometry the faster growing facet is expected to prevail [14,15]. This is in accordance with the ob-

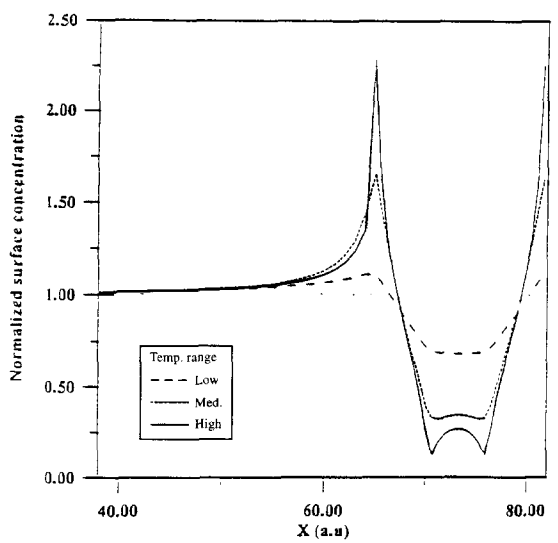

Fig. 3. Surface concentration profile across the IMG for the low (640°C), medium (720°C) and high (760°C) temperatures.

served $\{\bar{h}\bar{h}k\}A_{k>h}$ faceting where a high deposition rate should readily occur [16] because of the higher step densities associated with these surfaces. The maximally [16] stepped $\{\bar{1}\bar{1}3\}A$ surface would therefore be an optimal facet to develop along the bottom where the morphological importance of the faster growing face defines the crystal habit along the concave corner [14,15] of the IMG.

An explanation for the apparent stability of these facets is related to the formation of dimer bonds along the surface [17]. If complete surface reconstruction were to occur, by formation of dangling bonds along directions orthogonal ($R_\perp$) to the crystallographic step edge, then this would imply a maximum reduction of two out of the original three dangling bonds along the {001} treads of the $\{\bar{1}\bar{1}3\}A$ [18,19]. The $\{\bar{1}\bar{1}5\}A$ surface may also undergo a similar dimerization whereby three dangling bonds would remain, from the original five, if $R_\perp$ surface reconstruction were to occur [18].

Both $\{\bar{1}\bar{1}3\}A$ and $\{\bar{1}\bar{1}5\}A$ faces may also undergo reconstruction by dimer formation along the surface in a direction which is parallel ($R_\parallel$) to the {111} risers. In this case each surface atom on the {001} treads can form one dimer bond. For the $R_\perp$ reconstruction a rebonding of the step edge [17] results in a hybrid geometry [18], which gives an additional reduction of the dangling bond densities. This geometry is commensurate with double height steps [20] and is only possible for orientations from the {001} to the $\{\bar{1}\bar{1}5\}A$.

The conclusion that may be drawn from this discussion is that the $\{\bar{1}\bar{1}3\}A$ and $\{\bar{1}\bar{1}5\}A$ respectively represent the maximum reduction in dangling bond densities – i.e. minimization of surface energies – for the $R_\perp$ and hybrid geometries. In practice, however, stabilization in the far from equilibrium LP-OMVPE deposition of compound semiconductors will be determined by statistical mechanical concerns. Reconstruction will be related to surface conditions – i.e. surface coverages and process parameters like temperature [21]. Unreconstructed regions are expected to coexist with other possible dimer geometries [22] along the unequally spaced – i.e. different terrace widths [23,24] "step trains" related to the 2D step flow growth mechanism.

Decreased surface coverages favours dimer formation. This condition addresses the stability of the $\{\bar{h}\bar{h}k\}A_{k>h}$ faceting features. Upon increasing the growth temperatures – i.e. decreasing the supersaturation – the aforementioned facets acquire such a stable and slow growing rate, with respect to the side wall and {001} bottom, that they will no longer appear along the bottom corner of the IMG. The reason for this is related to bottom corner's concave configurations [14,15] where the faster growing faces will dictate the outcome of the developing crystal habit.

An interesting note is that experimentally the most prevalent faceting features, which arise during nonplanar growth of compound semiconductors, appear to be the {113} and {115} orientations (Fig. 1a and 1b) [9,25–27]. The significance of this is that these orientations may give rise to unique structures. For example, quantum dots [28,29], which results from exploring the Stranski–Krastonow growth mode, are features bounded by {113} type facets. Compositional gradients [30–32] might be used in order to laterally define a structure by doping levels which can be appreciably higher [33,34] than is ordinarily achieved on lower indexed faces. These structures might also be used to explore the segregation of various doping species in co-doped samples [25,35] or examine the amphoteric [36] character of Si in defining lateral p-n junctions.

4. Summary

The LP-OMVPE of GaInP on nonplanar {001} GaAs surfaces has been examined. It was found that the emerging crystal habit in the low temperature ($T < 720°C$) growth was characterized by faceting with lbrace $\{\bar{h}\bar{h}k\}A_{k>h}$ orientations. These features were correlated with computer simulations which determined an inversely proportional relation between the intra-groove supersaturation with temperature. The stability of the encountered facets were related to the possible surface reconstruction by the formation of dimer bonds.

Acknowledgements

P.L. Bastos gratefully acknowledges the financial support provided by CAPES and the fruitfull discussion with John Schermer.

References

[1] R. Bhat, M.A. Koza, M.J.S.P. Brasil, R.E. Nahory, C.J. Palmstrom and B.J. Wilkens, J. Crystal Growth 124 (1992) 576.

[2] F.E.G. Guimares, B. Elsner, R. Westphalen, B. Spangenberg, H.J. Geelen, P. Balk and K. Heime, J. Crystal Growth 124 (1992) 199.

[3] Y. Nomura, Y. Morishita, S. Goto and Y. Katayama, J. Electron. Mater. 23 (1994) 97.

[4] T. Fukui, S. Ando and Y.K. Fukai, Appl. Phys. Lett. 57 (1990) 1209.

[5] T. Fukui, S. Ando, T. Honda and T. Toriyama, Surf. Sci. 267 (1992) 236.

[6] Y. Sugiyama, Y. Sakuma, S. Muto and N. Yokoyama, Appl. Phys. Lett. 67 (1995) 256.

[7] D. Bertram, W. Stolz and E.O. Göbel, J. Crystal Growth 132 (1993) 179.

[8] T. Sogowa, S. Ando and H. Kanbe, Appl. Phys. Lett. 64 (1994) 472.

[9] R. Bhat, E. Kapon, S. Simhony, E. Colas, D.M. Hwang, N.G. Stoffel and M.A. Koza, J. Crystal Growth 107 (1991) 716.

[10] M.M.G. Bongers, P.L. Bastos, M.J. Anders and L.J. Giling, J. Crystal Growth, submitted.

[11] M.J. Anders, M.M.G. Bongers, P.L. Bastos and L.J. Giling, J. Crystal Growth 154 (1995) 240.

[12] C. Ratsch and A. Zangwill, Appl. Phys. Lett. 58 (1991) 403.

[13] K.M. Dzurko, S.G. Hummel, E.P. Menu and P.D. Dapkus, J. Electron. Mater. 19 (1990) 1367.

[14] S.H. Jones, L.K. Seidel, K.M. Lau and M. Harold, J. Crystal Growth 108 (1991) 73.

[15] H.E. Buckley, Crystal Growth (Wiley, New York, 1951).

[16] R.C. Sangster, Compound Semiconductors Vol. 1 (Reinhold, New York, 1962) p. 241.

[17] D.J. Chadi, Phys. Rev. B 29 (1984) 785.

[18] J.J. Schermer, W.J.P. van Enckevort and L.J. Giling, J. Crystal Growth 148 (1995) 248.

[19] P.L. Bastos, M.M.G. Bongers, M.J. Anders, J.J. Schermer and L.J. Giling, Surf. Sci. 344 (1995) L1275.

[20] D.J. Chadi, Phys. Rev. Lett. 59 (1987) 1691.

[21] A. Sakamoto, S. Otake, M. Yamamoto and I. Iwasa, J. Crystal Growth 145 (1994) 22.

[22] A.R. Avery, D.M. Holmes, T.S. Jones, B.A. Joyce and G.A.D. Briggs, Phys. Rev. B 50 (1994) 8098.

[23] K. Pond, R. Maboudian, V. Bressler-Hill, D. Leonard, X.S. Wang, K. Self, W.H. Weinberg and P.M. Petroff, J. Vac. Sci. Technol. B 11 (1993) 1374.

[24] M. Kasu and N. Kobayashi, J. Appl. Phys. 78 (1995) 3026.

[25] T. Takamori and T. Kamijoh, J. Appl. Phys. 77 (1995) 187.

[26] S.D. Hersee, E. Barbier and R. Blondeau, J. Crystal Growth 77 (1986) 310.

[27] P. Demeester, P. Van Daele and R. Baets, J. Appl. Phys. 63 (1988) 2284.

[28] W. Seifert, N. Carlsson, S. Jeppesen, M. Miller, M.E. Pistol and L. Samuelson, in: Proc. 6th Eur. Worshop on MOVPE, Gent, Belgium, June 1995, section C invited paper.

[29] Y. Nabetani, T. Ishikawa, S. Noda and A. Sasaki, J. Appl. Phys. 76 (1994) 347.

[30] M. Walther, E. Kapon, J. Chisten, D.M. Hwang and R. Bhat, Appl. Phys. Lett. 60 (1992) 521.

[31] G. Vermeire, I. Moerman, Z.Q. Yu, F. Vermaerke, P. van Daele and P. Demeester, J. Electron. Mater. 23 (1994) 121.

[32] A. Gustafsson, L. Samuelson, D. Hessman, J.-O. Malm, G. Vermeire and P. Demeester, J. Vac. Sci. Technol. B 13 (1995) 308.

[33] R. Bhat, C. Caneau, C.E. Zah, M.A. Koza, W.A. Bonner, D.M. Hwang, S.A. Schwarz, S.G. Menocal and F.G. Favire, J. Crystal Growth 107 (1991) 772.

[34] S. Minagawa, Y. Ishitani, T. Tanaka and S. Kawanaka, J. Crystal Growth 152 (1995) 251.

[35] C. Anayama, H. Sekiguchi, M Kondo, H. Sudo, T. Fukushima, A. Furuya and T. Tanahashi, Appl. Phys. Lett. 63 (1993) 1736.

[36] M. Henini, P.A. Crump, P.J. Rodgers, B.L. Gallagher, A.J. Vickers and G. Hill, J. Crystal Growth 150 (1995) 446.